# Synthesis, DNA-Binding and Photocleavage Studies of the Ruthenium(II) Complexes $[Ru(phen)_2(ppd)]^{2+}$ and $[Ru(phen)(ppd)_2]^{2+}$ (ppd = Pteridino[6,7-*f*][1,10]phenanthroline-11,13(10*H*,12*H*)-dione, phen = 1,10-Phenanthroline)

by **Feng Gao**[a]), **Hui Chao***[a])[b]), **Yuan-Fang Wei**[a]), **Yi-Xian Yuan**[a]), **Bin Peng**[a]), **Xin Chen**[a]), **Kang-Cheng Zheng**[a]), **Liang-Nian Ji***[a])

[a]) MOE Laboratory of Bioinorganic and Synthetic Chemistry, School of Chemistry and Chemical Engineering, Sun Yat-Sen University, Guangzhou 510275, P. R. China (fax: +86-20-84035497; e-mail: ceschh@mail.sysu.edu.cn)

[b]) State Key Laboratory of Coordination Chemistry, Nanjing University, Nanjing 210093, P. R. China

Two new complexes, $[Ru(phen)_2(ppd)]^{2+}$ (**1**) and $[Ru(phen)(ppd)_2]^{2+}$ (**2**) (ppd = pteridino[6,7-*f*][1,10]phenanthroline-11,13(10*H*,12*H*)-dione, phen = 1,10-phenanthroline) were synthesized and characterized by ES-MS, $^1$H-NMR spectroscopy, and elemental analysis. The intercalative DNA-binding properties of **1** and **2** were investigated by absorption-spectroscopy titration, luminescence-spectroscopy studies, thermal denaturation, and viscosity measurements. The theoretical aspects were further discussed by comparative studies of **1** and **2** by means of DFT calculations and molecular-orbital theory. Photoactivated cleavage of pBR322 DNA by the two complexes were also studied, and **2** was found to be a much better photocleavage reagent than **1**. The mechanism studies revealed that singlet oxygen and the excited-states redox potentials of the complex may play an important role in the DNA photocleavage.

**1. Introduction.** – The interaction of (polypyridine)ruthenium(II) complexes with DNA has attracted considerable interest during the past decades. An understanding of how these small molecules bind to DNA will be potentially useful in the design of new drugs and highly sensitive spectroscopic and reactive probes and diagnostic reagents [1–4]. However, the vast majority of such studies have focused on complexes with two ancillary ligands and one intercalative ligand, such as $[Ru(bpy)_2L]^{2+}$ and $[Ru(phen)_2L]^{2+}$ (bpy = 2,2′-bipyridine, phen = 1,10-phenanthroline) and, to a far lesser extent, on $Ru^{II}$ complexes with one ancillary ligand and two intercalating ligands [5–7]. In fact, the DNA-interaction properties of reported $[Ru(phen)L_2]^{2+}$ complexes are interesting for their diverse luminescence properties in both absence and presence of DNA. For example, $[Ru(phen)_2(pztp)]^{2+}$ (pztp = 3-(pyrazin-2-yl)-[1,2,4]triazino[5,6-*f*][1,10]phenanthroline) has been found to luminescence neither in aqueous buffer nor in the presence of DNA, while $[Ru(phen)(pztp)_2]^{2+}$ acts as an efficient 'DNA molecular light switch' [6]. Varying the number of intercalative ligands can create some interesting differences in the space configuration and the electron-density distribution of (polypyridine)ruthenium(II) complexes, which will result in some differences in spectral properties and the DNA-binding behaviors of the complexes, and will be helpful to more clearly understand the binding mechanism of $[Ru^{II}(polypyridine)]$ complexes to DNA.

Recently, we have designed and synthesized the dppz-like (dppz = dipyrido[3,2-*a*:2′3′-*c*]phenazine) ligand pteridino[6,7-*f*][1,10]phenanthroline-11,13(10*H*,12*H*)-dione (ppd). $[Ru(bpy)_2(ppd)]^{2+}$ was found to bind DNA with high affinity and act as a 'DNA molecular light switch' [8]. In this continuing study, two $Ru^{II}$ complexes $[Ru(phen)_2(ppd)]^{2+}$ (**1**) and $[Ru(phen)(ppd)_2]^{2+}$ (**2**) were synthesized and characterized. The DNA-binding properties of the two complexes were investigated by absorption-spectroscopy titration, emission-spectroscopy titration, competitive binding experiments with ethidium bromide (= 3,8-diamino-5-ethyl-6-phenylphenanthridinium bromide = EB), thermal-denaturation studies, viscosity measurements, and DFT calculations. The photocleavage behavior and mechanism of both complexes toward plasmid pBR322 DNA were also investigated. Results suggest that, although both **1** and **2** bind DNA *via* the intercalation mode, there are obvious differences in their light-switch behavior and DNA photocleavage.

**2. Results and Discussion.** – 2.1. *Synthesis and Characterization*. Similarly to the preparation of dppz, the ligand ppd was obtained by condensation of 1,10-phenanthroline-5,6-dione and 5,6-diaminouracil (*Scheme*). Complexes **1** and **2** were then synthesized by direct reaction of ppd with the appropriate mol ratios of the precursor complexes in ethylene glycol/$H_2O$. The desired $Ru^{II}$ complexes were isolated as their perchlorates and purified by column chromatography (alumina). The $^1$H-NMR data (*Exper. Part*) of **1** and **2** were consistent with the proposed structures. Similarly to other $Ru^{II}$ complexes [9][10], the resonances due to bound phen and ppd are shifted compared to those of free phen and ppd, indicating the complexation. Due to the shielding influences of the adjacent ppd and phen, the phen protons of complex **1** exhibit two distinct sets of signals. For the same reason, the ppd protons of complex **2** also give rise to two distinct sets of signals.

The absorption spectrum of complexes **1** and **2** show three well-resolved bands in the range 200–600 nm. The higher-energy bands at 365–380 nm are attributed to the $\pi-\pi^*$ transition, and the lower-energy bands at 453 and 449 nm are assigned to metal-ligand charge transfers (MLCTs). For both complexes **1** and **2**, two distinct MLCT bands, attributed to the $Ru(d\pi) \rightarrow phen(\pi^*)$ and $Ru(d\pi) \rightarrow ppd(\pi^*)$ transitions, respectively, might be expected. However, as a result of the broad nature of the bands and their relatively small wavelength separation, a broad MLCT band with a shoulder peak is observed in the spectra of these complexes. On excitation at 450 nm, the complexes **1** and **2** exhibit the characteristic emission band at 589 and 606 nm, respectively (*Table 1*). The emission intensity of **1** is over two times higher than that of **2**; however, the excited-state lifetime of **2** is longer than that of **1**. The reason of these differences is tentatively attributed to the different molecular-orbital energy levels of both the ground-state and the excited states of the two complexes. In $H_2O$, the absorption bands of both complexes are broader and accompanied by a slight blue shift. The steady-state emission of **1** and **2** is not observed in $H_2O$, due to quenching by $H_2O$ [13].

The electrochemical behaviors of the two complexes were determined in MeCN. Each complex exhibits one oxidation and three reduction waves in the sweep range from $-1.9$ to $+1.8$ V. The anodic and cathodic peak separations vary from 58 to 75 mV and are virtually independent of the scan rate, indicating that the processes are

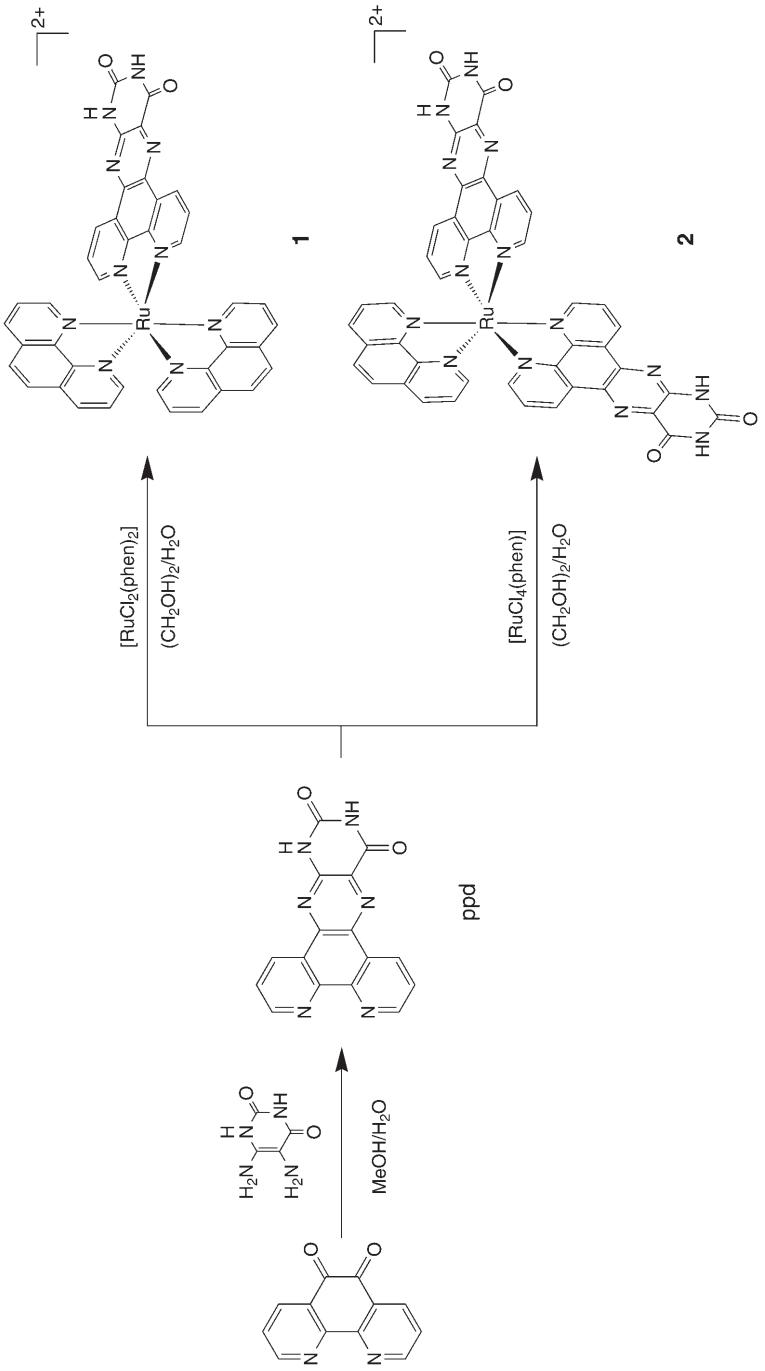


Scheme. *Synthesis of Ligand ppd and its Complexes* **1** *and* **2**

Table 1. *Emission Data for $Ru^{II}$ Complexes in MeCN at 298 K*

| | $\lambda_{em}$ [nm] | $\tau$ [ns] | $\Phi \cdot 10^3$ | Ref. |
|---|---|---|---|---|
| $[Ru(phen)_2(ppd)]^{2+}$ (**1**) | 589 | 239 | 6.7 | this work |
| $[Ru(phen)(ppd)_2]^{2+}$ (**2**) | 606 | 302 | 2.9 | this work |
| $[Ru(phen)_2(dppz)]^{2+}$[a]) | 630 | 180 | 21 | [11] |
| $[Ru(phen)_2(phehat)]^{2+}$[b]) | 662 | 191 | 11 | [12] |

[a]) dppz = dipyrido[3,2-*a* : 2′,3′-*c*]phenazine. [b]) phehat = 1,10-phenanthrolino[5,6-*b*]-1,4,5,8,9,12-hexaazatriphenylene = dipyrazino[2,3-*a* : 2′,3′-*c*]dipyrido[3,2-*h* : 2′,3′-*j*]phenazine.

reversible one-electron transfers. The electrochemical behavior of [$Ru^{II}$(polypyridine)] complexes has been rationalized in terms of a metal-based oxidation and a series of reductions which are ligand-based occurring in a stepwise manner for each $\pi^*$ system [14]. An oxidation wave corresponding to the $Ru^{III}/Ru^{II}$ couple was observed at 1.36 V for **1** and at 1.39 V for **2**, the oxidation potential shifting to a more positive value in accordance with the extension of the $\pi$ framework in **2**. A reduction wave for the complexed ppd of **1** occurs at $-1.27$ V, followed by the successive phen reductions at $-1.45$ and $-1.63$ V under similar experimental conditions. On the other hand, reduction of one ppd ligand of **2** occurs at $-0.98$ V, followed by the reduction of the other ppd and the phen ligand at $-1.14$ and $-1.56$ V. From the reduction behavior of **1** and **2**, we concluded that their LUMO $\pi^*$ orbitals are ppd-based and not phen-based.

The geometric molecular structures of complexes **1** and **2** were obtained by full geometry optimizations with the DFT method at the B3LYP/LanL2DZ level. The optimized structures of the complexes (*Fig. 1*) showed that the ppd ligand in **1** and **2** retains an excellent planarity, and the planar area is similar to that of dppz, confering to the two complexes higher DNA-binding abilities than those exhibited by most of the other $Ru^{II}$ complexes. The LUMO energy of **1** and **2** (*Fig. 1*) is lower than the HOMO energy of DNA. The DNA molecule is an electron donor, and the intercalated complex is the electron acceptor; therefore, it is easy to accept the electrons from DNA for **1** and **2**. The plots of the frontier MOs (*Fig. 1*) show that the HOMOs of both **1** and **2** are composed of orbitals from the central $Ru^{II}$ atom, and the LUMOs and LUMO + 1s are mostly composed of the MOs of ppd. Therefore, the LUMOs of the complexes are more prone to overlap with the HOMO of DNA when the complexes are intercalated into DNA base pairs. Both the energy and the distribution of the frontier MOs of the $Ru^{II}$ complexes **1** and **2** indicate that they may intercalate into the DNA base pairs with high affinity.

2.2. *DNA-Binding Studies.* For metallointercalators, DNA binding is associated with hypochromism and a red shift in the MLCT and ligand bands [15]. The absorption spectra of complexes **1** and **2** in the absence and presence of calf-thymus (CT) DNA at various complex concentrations are given in *Fig. 2*. As the concentration of DNA is increased, for complex **1**, the hypochromism in the MLCT band reaches a value as high as 29.7% at 425 nm, with a red shift of 12 nm at a ratio [DNA]/[Ru] of 10.0. For complex **2**, upon addition of DNA, the MLCT band at 429 nm exhibits hypochromism of *ca.* 23.3% with a 6 nm red shift at a ratio [DNA]/[Ru] of 11.0. These spectral characteristics suggest that there are interactions between the complexes and DNA.

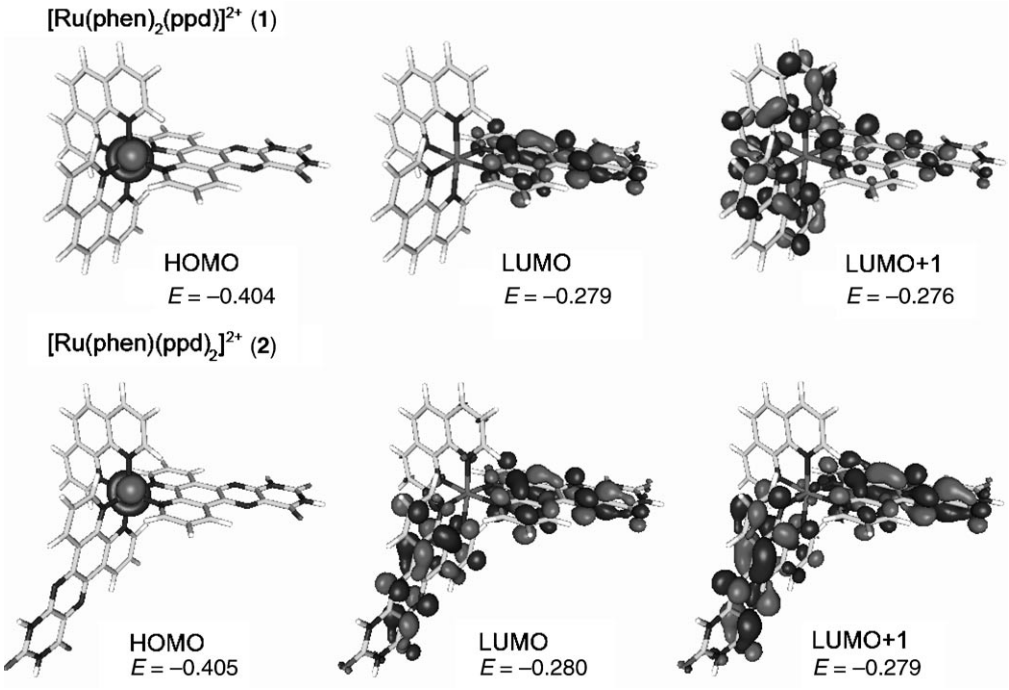


Fig. 1. *Contour plots and energies* E [a.u.] *of some related frontier molecular orbitals of complexes* **1** *and* **2**

The intrinsic binding constant $K_b$ of complexes **1** and **2** obtained were $(1.40 \pm 0.08) \cdot 10^6$ $M^{-1}$ ($s = 2.73 \pm 0.08$) and $(1.55 \pm 0.08) \cdot 10^6$ $M^{-1}$ ($s = 1.16 \pm 0.08$), respectively, from the decay of the absorbances [16]. The values are comparable to those of $[Ru(phen)_2(dppz)]^{2+}$ ($1 \cdot 10^6 - 5 \cdot 10^6$ $M^{-1}$) [11][13], which has similar ligand sizes and electronic structures, of $[Ru(phen)_2(phehat)]^{2+}$ ($2.5 \cdot 10^6$ $M^{-1}$) [12], of $[Ru(bpy)_2(tpphz)]^{2+}$ ($5.1 \cdot 10^6$ $M^{-1}$) [17], and of the representative DNA organic intercalator EB; $1.4 \cdot 10^6$ $M^{-1}$ [18] (phehat = dipyrazino[2,3-*a*:2′,3′-*c*]dipyrido[3,2-*h*:2′,3′-*j*]phenazine; tpphz = tetrapyrido[3,2-*a*:2′,3′-*c*:3″,2″-*h*:2‴,3‴-*j*]phenazine). These findings imply that **1** and **2** bind DNA in an intercalating mode by one ppd ligand intercalated between the adjacent DNA base pairs.

The intercalation of natural or synthesized organic compounds and metallointercalators generally results in a considerable increase in the melting temperature $T_m$ [19–21]. Here, DNA (100 μM) melting experiments revealed a $T_m$ of CT-DNA of $75.7 \pm 0.2°$ in the absence of a complex, while $T_m$ increased dramatically to $83.3 \pm 0.2°$ and $83.9 \pm 0.2°$ in the presence of **1** and **2** (10 μM), respectively (*Table 2*). The large increase (7.6–8.2°) in $T_m$ is comparable to that observed for classical intercalators [19–21]. The intrinsic DNA-binding constant $K_b$ at $T_m$ can be obtained from the *McGhee* equation. For the CT-DNA used in these studies, under identical solution conditions, a melting enthalpy $\Delta H_m$ of 6.9 kcal $mol^{-1}$ was determined by differential scanning calorimetry [22]. On the basis of the absorption-spectroscopy titration experiment, the values of $n$ for complex **1** and **2** were 2.76 and 1.73 bp (bp = base pairs). Thus $K_b$ was determined to

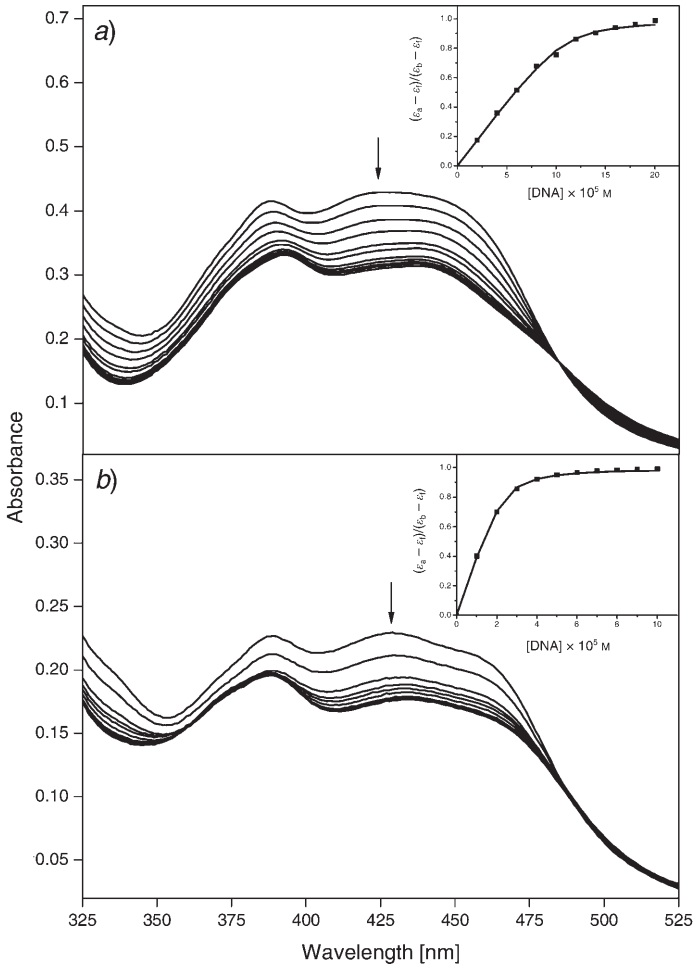


Fig. 2. *Absorption spectra of* a) *complex* **1** *in* Tris · *HCl buffer* A *in the presence of increasing amounts of CT-DNA* ([Ru] = 20 μM, [DNA] = 0–200 μM) *and* b) *complex* **2** *in* Tris · *HCl buffer* A *in the presence of increasing amounts of CT-DNA* ([Ru] = 10 μM, [DNA] = 0–110 μM). Buffer *A* = 5 mM *Tris* · HCl/50 mM NaCl, pH 7.0.

be $7.85 \cdot 10^4$ M$^{-1}$ at 83.3° for **1** and $3.03 \cdot 10^4$ M$^{-1}$ at 83.9° for **2** (*Table 2*). The standard enthalpy changes ($\Delta H^0$), standard entropy changes ($\Delta S^0$), and the standard free-energy changes ($\Delta G^0$) of the binding of **1** and **2** to CT-DNA were determined by *van't Hoff*'s equation [23] (*Table 2*). The negative $\Delta G^0$ value suggests that the energy of the complex–DNA adduct is lower than the sum of the energies of the free complex and DNA. The negative $\Delta H^0$ suggests that the binding of the complex to DNA at 25° is exothermic and driven by enthalpy. The negative entropy values indicate that the degree of freedom of the $Ru^{II}$ complexes is decreased after the binding, and that the DNA conformational freedom is also reduced upon complex–DNA binding.

Table 2. *Thermodynamic Parameters Estimated by the DNA Denaturation Study*

| | $[Ru(phen)_2(ppd)]^{2+}$ (**1**) | $[Ru(phen)(ppd)_2]^{2+}$ (**2**) |
|---|---|---|
| $T_m$ [°][a]) | 83.3 | 83.9 |
| $\Delta T_m$ [°] | 7.6 | 8.2 |
| $K_b$ at $T_m$ [M$^{-1}$] | $7.85 \cdot 10^4$ | $3.03 \cdot 10^4$ |
| $K_b$ at 25° [M$^{-1}$] | $1.40 \cdot 10^6$ | $1.55 \cdot 10^6$ |
| $\Delta G^0$ [kJ mol$^{-1}$][b]) | – 35.1 | – 35.3 |
| $\Delta H^0$ [kJ mol$^{-1}$] | – 43.7 | – 57.6 |
| $\Delta S^0$ [J mol$^{-1}$ K$^{-1}$] | – 28.8 | – 74.8 |

[a]) The $T_m$ of CT-DNA alone in SSC buffer (0.3M NaCl/0.03M sodium citrate) was 75.7°. [b]) The value of the standard free-energy change was set at 25°.

To further clarify the nature of the interaction between complexes **1** and **2** and DNA, viscosity measurements were carried out. A classical intercalation model demands that the DNA helix must lengthen as base pairs are separated to accommodate the binding ligand, leading to the increase of DNA viscosity [22][24]. The effects of complex **1** and **2**, together with those of $[Ru(bpy)_3]^{2+}$ and $[Ru(phen)_2(dppz)]^{2+}$, on the viscosity of rod-like DNA are shown in *Fig. 3*. $[Ru(phen)_2(dppz)]^{2+}$ increased the relative specific viscosity by lengthening of the DNA helix through the intercalation mode, while $[Ru(bpy)_3]^{2+}$, which has been known to bind with DNA in an electrostatic mode, exerted essentially no effect on DNA

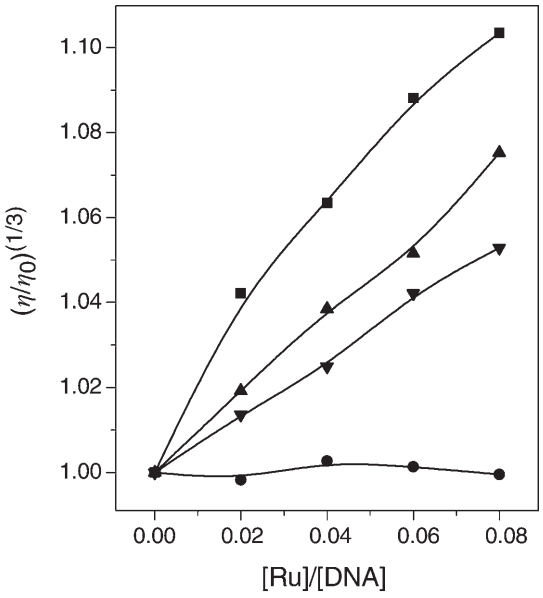


Fig. 3. *Effects of increasing amounts of complexes* **1** (▼) *and* **2** (▲), *compared with those of* $[Ru(bpy)_3]^{2+}$ (●) *and* $[Ru(phen)_2(dppz)]^{2+}$ (■), *on the relative viscosity of CT-DNA at* $28 \pm 1°$. $[CT\text{-}DNA]_{total} =$ 0.5 mM.

viscosity. On increasing the amounts of **1** and **2**, the relative viscosity of DNA increased steadily, similarly to the behavior of $[Ru(phen)_2(dppz)]^{2+}$. The increased degree of viscosity, which may depend on the affinity to DNA, follows the order $[Ru(phen)_2(dppz)]^{2+} > \mathbf{2} > \mathbf{1} > [Ru(bpy)_3]^{2+}$. These results suggest that **1** and **2** intercalate between the base pairs of DNA, which is consistent with the results of the absorption-spectroscopy titration and the thermal-denaturation studies.

2.3. *Light-Switch Behavior of the Ru$^{II}$ Complexes.* $[Ru(bpy)_2(dppz)]^{2+}$ and $[Ru(phen)_2(dppz)]^{2+}$ were reported to act as 'DNA molecular light switches'. These complexes exhibit nearly undetectable fluorescence in aqueous buffer, while intense luminescence is observed in the presence of DNA [25–28]. This fact was attributed to the protection of the N-atoms of the phenazine moiety from water as the dppz ligand in the complexes intercalated between adjacent base pairs of DNA. Ligand ppd is similar to dppz in size and electronic structure, and $[Ru(bpy)_2(ppd)]^{2+}$ has also been found to act as 'DNA molecular light switch' [8]. Therefore, luminescence studies of **1** and **2** are very useful to enhance the understanding of the luminescence properties and mechanism exhibited by (polypyridine)ruthenium(II) complexes, in view of the exploration of novel DNA sensitive luminescence probes and novel 'DNA molecular light switches'.

The emission spectra (*Fig. 4,a*) show that **1** hardly luminesced in *Tris*·HCl/NaCl buffer at room temperature in the absence of DNA. Upon addition of CT-DNA, the emission intensity of **1** increased greatly by a factor of *ca.* 20, which is higher than those observed for most $[Ru(phen)_2L]^{2+}$ complexes reported so far [11][29–31]. The increase of emission intensity also implies that **1** strongly interacts with DNA and is efficiently protected by DNA from the solvent $H_2O$ molecules, and that the complex

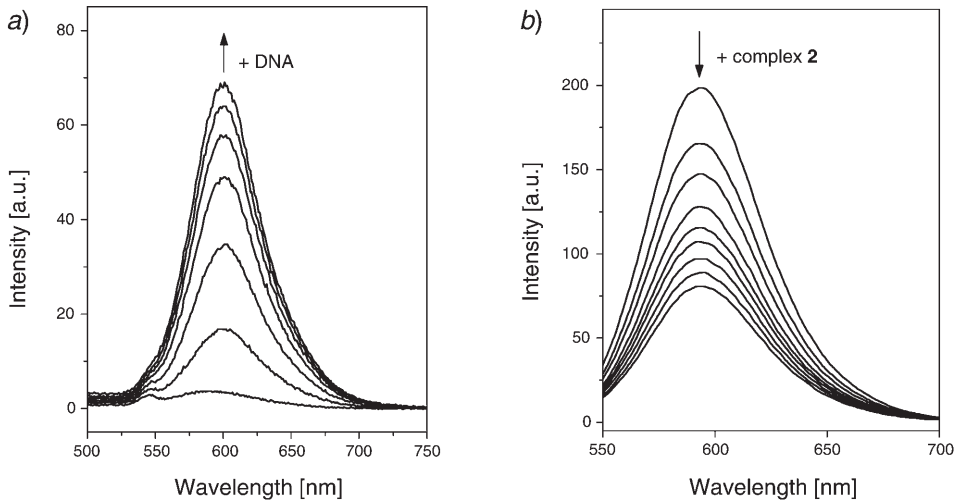


Fig. 4. a) *Emission spectra of complex* **1** *in 5 m*M Tris·*HCl/50 m*M *NaCl buffer* (pH 7.0): *intensity increase with increasing CT-DNA concentration* (intensity *ca.* 0 in the absence of CT-DNA). b) *Emission spectra of EB-bound CT-DNA* ([EB] = 1.0 μM, [CT-DNA] = 20.0 μM): *intensity decrease with increasing concentration of complex* **2** *from 0 to 3.2* μM.

mobility is restricted at the binding site, leading to a decrease of the vibrational modes of relaxation.

In the case of complex **2**, although its emission intensity in aqueous buffer is similar to that of **1**, the emission intensity only increased by a factor of *ca.* 1.5 upon addition of CT-DNA. This can be understood on the grounds that only one ppd ligand of **2** intercalates between the DNA base pairs, while the other remains exposed to the buffer. Thus, the N-atoms of the pteridine moiety of this external ppd ligand are still accessible to $H_2O$, and the luminescence of the complex was quenched. For complexes exhibiting weak emission intensity and a small enhancement in presence of DNA, competitive binding to DNA of the complexes with EB provides rich information regarding the DNA-binding nature and relative DNA-binding affinity [32][33]. EB emits intense fluorescence in the presence of DNA, due to its strong intercalation between the adjacent DNA base pairs [18]. If this enhanced fluorescence is quenched, at least partially, by addition of a second intercalative molecule, this will be an evidence of the intercalation of the second molecule. The intensity decrease in the emission spectrum of EB-bound CT-DNA on addition of increasing amounts of **2** indicated that **2** intercalated between the base pairs of DNA, thus replacing EB molecules (*Fig. 4,b*).

2.4. *DNA Photocleavage.* There is substantial and continuing interest in DNA endonucleolytic cleavage reactions that are activated by metal ions [34–36]. *Fig. 5* shows gel-electrophoresis separations of pBR322 DNA after incubation with complex **1** or **2** and irradiation at 365 nm for 60 min. No DNA cleavage was observed in the control experiments in which the complex was absent (*Lane 0*). With increasing concentration of the $Ru^{II}$ complexes (*Lanes 1–4* and *5–8*), the amount of *Form I* (supercoil form) of pBR322 DNA diminished gradually, whereas *Form II* (nicked form) increased. At 20 μM, complex **2** promoted an almost complete conversion from *Form I* to *Form II* (*Lane 8*), while complex **1** induced only 8% of pBR322 DNA cleavage (*Lane 1*). Thus, complex **2** is a better DNA photocleavage reagent than complex **1**.

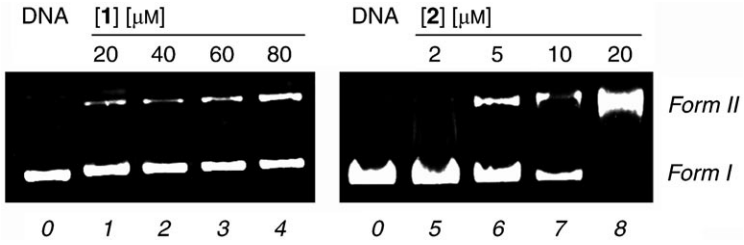


Fig. 5. *Gel electrophoresis after photoactivated cleavage of pBR322 DNA by different concentrations of $Ru^{II}$ complexes* **1** (*Lanes 1–4*) *or* **2** (*Lanes 5–8*), *on irradiation at 365 nm for 60 min*

Whether a higher photoactived-DNA-cleavage efficiency of a certain [$Ru^{II}$(polypyridine)] complex originates from its more favorable DNA-binding ability is still matter of dispute. To determine the reactive species responsible for the photoactivated cleavage of the plasmid and to establish the cleavage mechanism, the following experiments were carried out. Photoactivated cleavage of pBR322 DNA in the presence of $Ru^{II}$ complex **1** or **2** and different inhibitors is shown in *Fig. 6*, together with

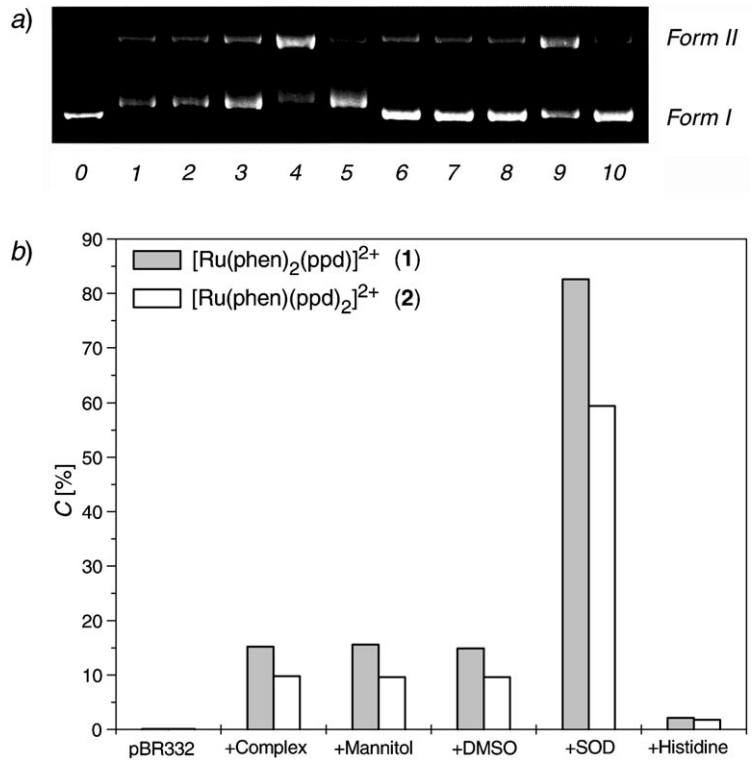


Fig. 6. a) *Gel electrophoresis after photoactivated cleavage of pBR322 by complexes* **1** *or* **2** *in the presence of different inhibitors, on irradiation at 365 nm for 60 min and* b) *bar diagram of the percentage of cleavage* (*C*) *in the presence of the inhibitors. Lane 0*, no complex; *Lanes 1* and *6*, in the presence of **1** (40 μM) or **2** (10 μM), no inhibitors; *Lanes 2–5* and *7–10*, in the presence of complex and different inhibitors; *Lanes 2* and *7*, mannitol (100 mM); *Lanes 3* and *8*, DMSO (200 mM); *Lanes 4* and *9*, superoxide dismutase (= SOD; 1 U/μl); *Lanes 5* and *10*, histidine (1.2 mM).

the bar diagram of the percentage of cleavage (*C*) in the presence of the inhibitors. For both complexes, the cleavage of the plasmid was not inhibited in the presence of hydroxyl-radical (OH$^{\bullet}$) scavengers such as mannitol [37] and DMSO [38] even at high concentration, indicating that OH$^{\bullet}$ was not likely to be the cleaving agent. While in the presence of superoxide dismutase (SOD), a facile superoxide anion radical ($O_2^{\bullet-}$) quencher, the cleavage was obviously improved, which indicated that $O_2^{\bullet-}$ might be an inhibitor of the photoactivated cleavage of the plasmid and reducing the amount of $O_2^{\bullet-}$ can improve the cleavage effect. SOD strongly enhancing the yield of cleavage has also been observed in the photoactivated cleavage of other compounds [8][39–41]. Moreover, the DNA cleavage of the plasmid by either **1** or **2** was inhibited in the presence of the singlet-oxygen ($^1O_2$) scavenger histidine [42], suggesting that $^1O_2$ is likely to be the reactive species responsible for the cleavage reaction. Similar cases have been observed in the DNA photocleavage by $[Ru(phen)_3]^{2+}$ which is attributed to an $^1O_2$-based mechanism [43]. Although the reactive species modulating the DNA

photocleavage was found to be in accordance with that of **2**, **1** exhibited less DNA-cleavage activity than **2**. The different DNA-cleavage activity is related to the different $^1O_2$-producing efficiency and the excited-state lifetime.

To establish the $^1O_2$-generation abilities of $Ru^{II}$ complexes, the $^1O_2$ generation quantum yield ($\Phi_\Delta$) of each complex was calculated according to *Eqns. 1* and *2*, where $I_{in}$ is the incident monochromatic light intensity, $\Phi_{ab}$ is the light-absorbing efficiency of the photosensitizer, $\Phi_r$ is the reaction quantum yield of $^1O_2$ with 1,3-diphenylisobenzofuran (DPBF), $t$ is the irradiation time, $I_0$ and $I_t$ are the fluorescence intensities of DPBF before and after irradiation, $k$ is the slope, and superscript s stands for standard. With $[Ru(bpy)_3]^{2+}$ as standard ($\Phi^s_\Delta = 0.81$ [44]), the $\Phi_\Delta$ of complexes **1**, **2**, and $[Ru(bpy)_2(dppz)]^{2+}$ were calculated to be 0.37, 0.50, and 0.09, respectively (*Fig. 7*). The $^1O_2$-generation quantum yield of the complexes follow the order $[Ru(bpy)_3]^{2+} > \mathbf{2} > \mathbf{1} > [Ru(bpy)_2(dppz)]^{2+}$, which is in accord with their DNA-photocleavage ability.

$$\frac{-\Delta[\mathrm{DPBF}]}{t} = \frac{I_0 - I_t}{t} = I_{in}\Phi_{ab}\Phi_\Delta\Phi_r \tag{1}$$

$$\frac{k}{k^s} = \frac{\Phi_{ab}}{\Phi^s_{ab}} = \frac{\Phi_\Delta}{\Phi^s_\Delta} \tag{2}$$

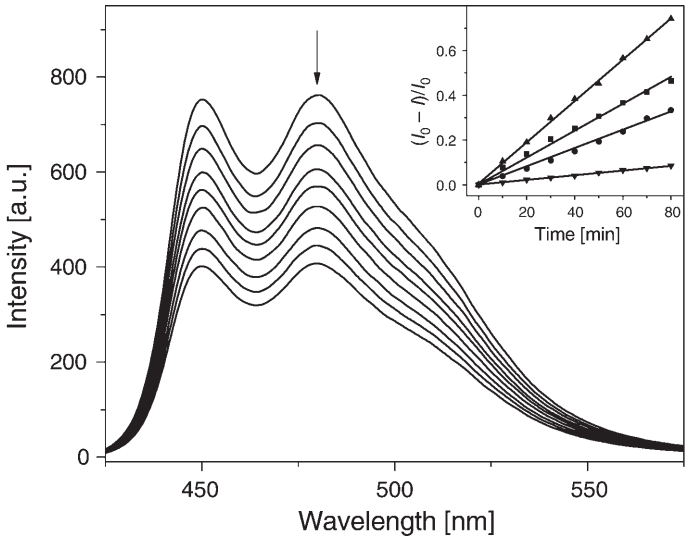


Fig. 7. *Emission spectra changes of the DPBF/complex* **2** *system upon irradiation at 365 nm with increasing concentration of* **2**. Inset: the DPBF consumption percentage as a function of irradiation time in the air-equilibrated MeOH solution of complex **1** (■), **2** (●), $[Ru(bpy)_3]^{2+}$ (▲), and $[Ru(bpy)_2(dppz)]^{2+}$ (▼).

Moreover, the fact that the DNA-photoactivated-cleavage activity under Ar (*Fig. 8*) is lower than that in air also suggests that, besides the reactive oxygen species, a direct oxidative process may contribute to the cleavage. Photoinduced electron transfer from the guanine to the excited complex has been demonstrated as the primary process,

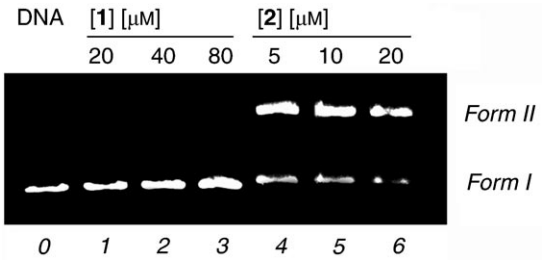


Fig. 8. *Gel electrophoresis after photoactivated cleavage of pBR322 DNA by different concentrations of* $Ru^{II}$ *complexes* **1** (*Lanes 1–3*) *and* **2** (*Lanes 4–6*) *under Ar, on irradiation at 365 nm for 60 min*

which initiates DNA cleavages [45]. Briefly, making the complex more oxidizing in the excited state will accelerate the electron-transfer process, thus will promote the DNA cleavages. The redox potentials for the ground and excited states (estimated from the lowest limit of the $\Delta E_{00}$ energy, *i.e.*, the emission maximum) of the two complexes together with similar complexes are compared in *Table 3*. The redox potentials of the excited states show that $[Ru(phen)(ppd)_2]^{2+*}$ (**2***) is slightly more oxidizing than $[Ru(phen)_2(ppd)]^{2+*}$ (**1***) and other complexes in *Table 3*. Therefore, a more efficient photoinduced electron transfer may be another factor contributing to the higher photocleavage activity of **2**. However, the redox potentials for the excited states should be regarded as approximations because the orbitals involved in the spectroscopy and electrochemistry are different.

Table 3. *Electrochemical Data for the* $Ru^{II}$ *Complexes in the Ground and Excited States*

| | $E_{ox}$ [V] | $E_{red}$ [V][a]) | $E_{ox}$* [V] | $E_{red}$*[V] | Ref. |
|---|---|---|---|---|---|
| $[Ru(phen)_2(ppd)]^{2+}$ (**1**[b]) | +1.36 | −1.27 | −0.75 | +0.84 | this work |
| $[Ru(phen)(ppd)_2]^{2+}$ (**2**[b]) | +1.39 | −0.98 | −0.72 | +1.13 | this work |
| $[Ru(phen)_2(dppz)]^{2+}$ | +1.30 | −1.00 | −0.67 | +0.96 | [11][13] |
| $[Ru(phen)_2(phehat)]^{2+}$ | +1.35 | −0.84 | −0.55 | +1.10 | [12] |
| $[Ru(phen)_3]^{2+}$ | +1.27 | −1.35 | | | [46] |

[a]) Potential of the first reduction wave. [b]) All complexes were measured in 0.1M $(Bu_4N)ClO_4$/MeCN; error in potentials was ±0.02 V; *T* 23 ± 1°; scan rate 100 $mV \cdot s^{-1}$.

**3. Conclusion.** – Studies on the DNA interaction of $Ru^{II}$ complexes with two intercalating ligands are very rarely reported. Here, a pair of complexes, $[Ru(phen)_2(ppd)]^{2+}$ (**1**) and $[Ru(phen)(ppd)_2]^{2+}$ (**2**), were synthesized and characterized by various physical methods. Both experimental and theoretical-calculation results suggest that the two complexes **1** and **2** bind to DNA in an intercalative mode, and the complex **2** with two intercalating ligands binds DNA more tightly. Luminescence studies reveal that **1** is a moderate 'DNA molecular light switch', while **2** is nearly nonluminescent in the absence and presence of DNA. Both complexes can induce DNA cleavage upon irradiation, and the DNA-photocleavage activity of **2** is much higher than that of **1**. The mechanism studies reveal that the singlet oxygen and

the excited-states redox potentials of the complexes play an important role in the DNA photocleavage.

We gratefully acknowledge support from the *National Natural Science Foundation of China*, the *973 Program*, the *Program for New Century Excellent Talents in University*, the *Scientific Research Foundation for the Returned Overseas Chinese Scholars of Ministry of Education*, and the *State Key Laboratory of Coordination Chemistry* at Nanjing University.

## Experimental Part

*General.* The compounds 1,10-phenanthroline-5,6-dione [47], *cis*-[Ru(phen)$_2$Cl$_2$]·2 H$_2$O [48], [Ru(phen)Cl4][49], and ppd [8] were prepared and characterized according to literature procedures. Other reagents and solvents were purchased and used without further purification unless otherwise noted. Calf-thymus DNA (CT-DNA) was obtained from *Sigma*. The dialysis membrane was purchased from *Union Carbide Co.* and treated by means of the general procedure before use [50]. A soln. of CT-DNA in the buffer *A* (= 5 mM *Tris*·HCl/50 mM NaCl, pH 7.0; *Tris* = tris(hydroxymethyl)amino-methane = 2-amino-2-(hydroxymethyl)propane-1,3-diol) gave a ratio of UV absorbance at 260 and 280 nm of 1.8–1.9 : 1, indicating that the DNA was sufficiently free of protein [51]. The DNA concentration per nucleotide was determined by absorption spectroscopy by using the molar absorption coefficient (6600 M$^{-1}$ cm$^{-1}$) at 260 nm [52]. Viscosity measurements: *Ubbelodhe* viscometer maintained at 28.0 ± 0.1° (thermostatic bath); DNA samples of *ca.* 200 base pairs in average length, sonicated to minimize complexities arising from DNA flexibility [53]; flow time measured with a digital stopwatch 3 × for each sample, the average value was used; data presented as $(\eta/\eta_0)^{1/3}$ *vs.* binding ratio [54], where $\eta$ is the viscosity of DNA in the presence of complexes and $\eta_0$ is the viscosity of DNA alone. Cyclic voltammetry: *Autolab-PGSTAT30* electrochemical system; supporting electrolyte, 0.1M ($Bu_4N$)$ClO_4$ in MeCN, freshly distilled from $P_2O_5$ and deaerated by purging with $N_2$ at r.t. Electrochemical measurements: typical cell, with a Pt-wire working electrode, a Pt flat counter electrode, and a standard sat. sodium chloride calomel electrode (SSCE). UV/VIS Spectra: *Perkin-Elmer-Lambda-850* spectrophotometer. Steady-state emission measurements: *Perkin-Elmer-LS 55* spectrofluorophotometer; at r.t. Time-resolved emission measurements: *FLS-920* spectrometer for combined fluorescence-lifetime and steady-state fluorescence measurements; excitation wavelength 450 nm, emission decay observed at 590 nm. $^1$H-NMR Spectra: *Varian-Inova-500NB* NMR spectrometer; $(CD_3)_2SO$ as solvent, at r.t.; chemical shifts $\delta$ in ppm rel. to $SiMe_4$. Electrospray mass spectra (ES-MS): *LCQ* system (*Finnigan MAT*, USA); quoted *m*/*z* values for the major peaks in the isotope distribution. Elemental analyses (C, H, and N): *Perkin-Elmer-240Q* elemental analyzer.

*(Pteridino[6,7-f][1,10]phenanthroline-11,13(10*H,*12*H*)-dione-*κN$^4$,*κN$^5$*)bis(1,10-phenanthroline-*κN$^1$,*κN$^{10}$*)ruthenium(II) Diperchlorate Dihydrate* ([Ru(phen)$_2$(ppd)](ClO$_4$)$_2$·2 H$_2$O; **1**·2 ClO$_4^-$·2 H$_2$O). A mixture of *cis*-[Ru(phen)$_2$Cl$_2$]·2 H$_2$O (0.284 g, 0.5 mmol), ppd (0.095 g, 0.3 mmol), ethylene glycol (16 ml), and H$_2$O (4 ml) was heated at 120° under Ar for 6 h (→ dark red soln.). The soln. was cooled and diluted with H$_2$O (40 ml). The product was precipitated by dropwise addition of sat. aq. NaClO$_4$ soln., collected by filtration, and purified by column chromatography (CC; alumina, EtOH/MeCN 4 : 1). The deep red product was further recrystallized from MeCN/Et$_2$O and dried *in vacuo:* 0.435 g (86%) of **1**·2 ClO$_4^-$·2 H$_2$O. $^1$H-NMR ($(CD_3)_2SO$): 10.89 (br., 2 H); 8.83 (*d*, *J* = 8.0, 2 H); 8.70 (*d*, *J* = 8.0, 2 H); 8.74 (*d*, *J* = 8.0, 2 H); 8.39 (*m*, 6 H); 8.06 (*d*, *J* = 8.0, 4 H); 7.84 (*d*, *J* = 8.0, 2 H); 7.74 (*t*, 4 H). ES-MS (MeCN): 777.5 ([*M* − 2 ClO$_4$ − H]$^+$), 389.2 ([*M* − 2 ClO$_4$]$^{2+}$). Anal. calc. for $C_{40}H_{24}Cl_2N_{10}O_{10}Ru$·2 H$_2$O: C 47.44, H 2.79, N 13.83; found: C 47.12, H 2.91, N 13.62.

*Bis(pteridino[6,7-f][1,10]phenanthroline-11,13(10*H,*12*H*)-dione-*κN$^4$,*κN$^5$*)(1,10-phenanthroline-*κN$^1$,*κN$^{10}$*)ruthenium(II) Diperchlorate Dihydrate* ([Ru(phen)(ppd)$_2$](ClO$_4$)$_2$·2 H$_2$O; **2**·2 ClO$_4^-$·2 H$_2$O). As described for **1**·2 ClO$_4^-$·2 H$_2$O, with [Ru(phen)Cl$_4$] (0.05 g, 0.12 mmol), ppd (0.095 g, 0.3 mmol), ethylene glycol (19 ml), and H$_2$O (1 ml) at 140° for 10 h. CC (alumina, MeOH) gave a red product which was recrystallized from MeOH/Et$_2$O and dried *in vacuo:* 0.043 g (32%) of **2**·2 ClO$_4^-$·2 H$_2$O. $^1$H-NMR ($(CD_3)_2SO$): 11.30 (br., 4 H); 9.22 (*d*, *J* = 8.0, 4 H); 8.78 (*d*, *J* = 8.0, 2 H); 8.39 (*d*, *J* = 8.0, 2 H); 8.21 (*d*, *J* = 8.0, 2 H); 8.12 (*d*, *J* = 8.0, 2 H); 7.99 (*d*, *J* = 8.0, 2 H); 7.79 (*m*, 6 H). ES-MS (MeCN):

914.1 ($[M-2\,ClO_4-H]^+$), 457.1 ($[M-2\,ClO_4]^{2+}$). Anal. calc. for $C_{44}H_{24}Cl_2N_{14}O_{12}Ru\cdot 2\,H_2O$: C 46.00, H 2.46, N 17.07; found: C 45.76, H 2.81, N 16.78.

*DNA Photocleavage Experiments.* For the gel electrophoresis experiment, supercoiled pBR322 DNA (0.1 μg) was treated with the $Ru^{II}$ complex in the *Tris*·HCl buffer *B* (= 50 mM *Tris*·HCl/18 mM NaCl, pH 7.2). The soln. was then irradiated at r.t. with a UV lamp (365 nm, 10 W). The sample was analyzed by electrophoresis for 1.5 h at 70 V on a 1% agarose gel in TBE buffer (= 89 mM *Tris*·boric acid/2 mM EDTA, pH 8.3). The gel was stained with 1 $\mu g\cdot ml^{-1}$ of EB, photographed, and analyzed by an *Alpha-Innotech-IS-5500* imaging system.

*Quantum Yield of $^1O_2$ Generation.* A series of 2 ml of air-saturated MeOH solns. containing DPBF (20 μM) and a complex (40 μM) were separately charged into an open 1 cm path fluorescence cuvette and illuminated with light of 365 nm (obtained from a *Perkin-Elmer-LS-55* fluorescence spectrophotometer, 10 nm of excitation slit width). The consumptions of DPBF were followed by monitoring its fluorescence-intensity decrease at the emission maximum ($\lambda_{ex}$ 405 nm, $\lambda_{em}$ 479 nm) at different irradiation times [55].

*Theoretical Calculations.* The DFT calculations were carried out with the Gaussian98 quantum-chemistry program package [56] by using *Becke*'s three-parameter hybrid functional (B3LYP) method [57–60] and the LanL2DZ basis set (a double-zeta basis set containing effective core potential) [60–62]. The full geometry-optimization computations were carried out for the ground states (singlet state) of the complexes [63]. The stability of the optimized conformation of the complexes was confirmed by the frequency analysis, which shows no imaginary frequency for each energy minimum. To vividly depict the detail of the frontier molecular orbital of the complexes, the stereographs of some related molecular orbitals were visualized based on the computational results.

## REFERENCES

[1] 'Metal Ions in Biological Systems', Vol. 33, Eds. A. Sigel and H. Sigel, Marcel Dekker, New York, 1996.
[2] K. E. Erkkila, D. T. Odom, J. K. Barton, *Chem. Rev.* **1999**, *99*, 2777; C. Metcalfe, J. A. Thomas, *Chem. Soc. Rev.* **2003**, *32*, 215; M. J. Clarke, *Coord. Chem. Rev.* **2003**, *236*, 209; B. Elias, A. Kirsch-De Mesmaeker, *Coord. Chem. Rev.* **2006**, *250*, 1627.
[3] Y. Xiong, L. N. Ji, *Coord. Chem. Rev.* **1999**, *185–186*, 711; L. N. Ji, X. H. Zou, J. G. Liu, *Coord. Chem. Rev.* **2001**, *216–217*, 513; H. Chao, L. N. Ji, *Bioinorg. Chem. Appl.* **2003**, *3*, 15.
[4] M. Eriksson, M. Leijon, C. Hiort, B. Nordén, A. Graslund, *J. Am. Chem. Soc.* **1992**, *114*, 4933; C. G. Coates, L. Jacquet, J. J. McGarvey, S. E. J. Bell, A. H. R. Al-Obaidi, J. M. Kelly, *J. Am. Chem. Soc.* **1997**, *119*, 7130; B. Önfelt, P. Lincoln, B. Nordén, *J. Am. Chem. Soc.* **2001**, *123*, 3630; J. A. Smith, J. L. Morgan, A. G. Turley, J. G. Collins, F. R. Keene, *Dalton Trans.* **2006**, 3179; D. L. Ma, C. M. Che, F. M. Siu, M. Yang, K. Y. Wong, *Inorg. Chem.* **2007**, *46*, 740.
[5] A. Ambroise, B. G. Maiya, *Inorg. Chem.* **2000**, *39*, 4264.
[6] X. H. Zou, B. H. Ye, H. Li, Q. L. Zhang, H. Chao, J. G. Liu, L. N. Ji, *J. Biol. Inorg. Chem.* **2001**, *6*, 143.
[7] B. Y. Wu, L. H. Gao, Z. M. Duan, K. Z. Wang, *J. Inorg. Biochem.* **2005**, *99*, 1685.
[8] F. Gao, H. Chao, F. Zhou, Y. X. Yuan, B. Peng, L. N. Ji, *J. Inorg. Biochem.* **2006**, *100*, 1487.
[9] K. J. Black, H. Huang, S. High, L. Starks, M. Olson, M. E. McGuire, *Inorg. Chem.* **1993**, *32*, 5591.
[10] Y. J. Liu, H. Chao, J. H. Yao, H. Li, Y. X. Yuan, L. N. Ji, *Helv. Chim. Acta* **2004**, *87*, 3119.
[11] R. M. Hartshorn, J. K. Barton, *J. Am. Chem. Soc.* **1992**, *114*, 5919.
[12] C. Moucheron, A. Kirsch-De Mesmaeker, S. Choua, *Inorg. Chem.* **1997**, *36*, 584.
[13] A. E. Friedman, J. C. Chambron, J. P. Sauvage, N. J. Turro, J. K. Barton, *J. Am. Chem. Soc.* **1990**, *112*, 4960.
[14] S. Zails, V. Drchal, *Chem. Phys.* **1987**, *118*, 313.
[15] A. M. Pyle, J. P. Rehmann, R. Meshoyrer, C. V. Kumar, N. J. Turro, J. K. Barton, *J. Am. Chem. Soc.* **1989**, *111*, 3051.
[16] M. T. Carter, M. Rodriguez, A. Bard, *J. Am. Chem. Soc.* **1989**, *111*, 8901.

[17] Y. Liu, A. Chouai, N. N. Degtyareva, D. A. Lutterman, K. R. Dunbar, C. Turro, *J. Am. Chem. Soc.* **2005**, *127*, 10796.
[18] J. B. Le Pecq, C. Paoletti, *J. Mol. Biol.* **1967**, *27*, 87.
[19] M. J. Waring, *J. Mol. Biol.* **1965**, *13*, 269.
[20] G. A. Neyhart, N. Grover, S. R. Smith, W. A. Kalsbeck, T. A. Fairly, M. Cory, H. H. Thorp, *J. Am. Chem. Soc.* **1993**, *115*, 4423.
[21] F. Gao, H. Chao, F. Zhou, L. C. Xu, K. C. Zheng, L. N. Ji, *Helv. Chim. Acta* **2007**, *90*, 36.
[22] S. Satyanarayana, J. C. Dabrowiak, J. B. Chaires, *Biochemistry* **1993**, *32*, 2573.
[23] H. Q. Liu, B. C. Tzeng, Y. S. You, S. M. Peng, H. L. Chan, M. Yang, C. M. Che, *Inorg. Chem.* **2002**, *41*, 3161.
[24] S. Satyanarayana, J. C. Dabrowiak, J. B. Chaires, *Biochemistry* **1992**, *31*, 9319.
[25] C. Hiort, P. Lincoln, B. Nordén, *J. Am. Chem. Soc.* **1993**, *115*, 3448.
[26] I. Haq, P. Lincoln, D. Suh, B. Nordén, B. Z. Chowdhry, J. B. Chaires, *J. Am. Chem. Soc.* **1995**, *117*, 4788.
[27] C. Turro, S. H. Bossmann, Y. Jenkins, J. K. Barton, N. J. Turro, *J. Am. Chem. Soc.* **1995**, *117*, 9026.
[28] R. B. Nair, B. M. Cullum, C. J. Murphy, *Inorg. Chem.* **1997**, *36*, 962.
[29] Q. X. Zhen, Q. L. Zhang, J. G. Liu, B. H. Ye, L. N. Ji, L. Wang, *J. Inorg. Biochem.* **2000**, *78*, 293.
[30] H. Xu, K. C. Zheng, H. Deng, L. J. Lin, Q. L. Zhang, L. N. Ji, *New J. Chem.* **2003**, *27*, 1255.
[31] L. F. Tan, H. Chao, H. Li, Y. J. Liu, B. Sun, W. Wei, L. N. Ji, *J. Inorg. Biochem.* **2005**, *99*, 513.
[32] B. C. Baguley, M. Lebret, *Biochemistry* **1984**, *23*, 937.
[33] J. R. Lakowicz, G. Webber, *Biochemistry* **1973**, *12*, 4161.
[34] D. S. Sigman, *Acc. Chem. Res.* **1986**, *19*, 180.
[35] S. Sitlani, E. C. Long, A. M. Pyle, J. K. Barton, *J. Am. Chem. Soc.* **1992**, *114*, 2303.
[36] J. K. Barton, A. L. Raphael, *J. Am. Chem. Soc.* **1984**, *106*, 2466.
[37] C. C. Cheng, S. E. Rokita, C. J. Burrows, *Angew. Chem., Int. Ed.* **1993**, *32*, 277.
[38] S. A. Lesko, R. J. Lorentzen, P. O. Ts'o, *Biochemistry* **1980**, *19*, 3023.
[39] F. Gao, H. Chao, J. Q. Wang, Y. X. Yuan, B. Sun, Y. F. Wei, B. Peng, L. N. Ji, *J. Biol. Inorg. Chem.* **2007**, *12*, 1015.
[40] S. Y. Kim, O. J. Kwon, J. W. Park, *Biochimie*, **2001**, *83*, 437.
[41] L. Bijeire, B. Elias, J. P. Souchard, E. Gicquel, C. Moucheron, A. Kirsch-De Mesmaeker, P. Vicendo, *Biochemistry* **2006**, *45*, 6160.
[42] R. Nilsson, P. B. Merkel, D. R. Kearns, *Photochem. Photobiol.* **1972**, *16*, 117.
[43] H. Y. Mei, J. K. Barton, *Proc. Natl. Acad. Sci. U.S.A.* **1988**, *85*, 1339.
[44] A. A. Abdel-Shafi, P. D. Beer, R. J. Mortimer, F. Wilkinson, *J. Phys. Chem. A* **2000**, *104*, 192.
[45] J. P. Lecomte, A. Kirsch-De Mesmaeker, A. B. Tossi, J. M. Kelly, H. Görner, *Photochem. Photobiol.* **1992**, *55*, 681.
[46] F. Barigelletti, A. Juris, V. Balzani, P. Belser, A. von Zelewsky, *Inorg. Chem.* **1987**, *26*, 4115.
[47] M. Yamada, Y. Tanaka, Y. Yoshimato, S. Kuroda, I. Shimao, *Bull. Chem. Soc. Jpn.* **1992**, *65*, 1006.
[48] B. P. Sullivan, D. J. Salmon, T. J. Meyer, *Inorg. Chem.* **1978**, *17*, 3334.
[49] R. A. Krause, *Inorg. Chim. Acta.* **1977**, *22*, 209.
[50] J. K. Barton, J. J. Dannenberg, A. L. Raphael, *J. Am. Chem. Soc.* **1984**, *106*, 2172.
[51] J. Marmur, *J. Mol. Biol.* **1961**, *3*, 208.
[52] M. E. Reichmann, S. A. Rice, C. A. Thomas, P. Doty, *J. Am. Chem. Soc.* **1954**, *76*, 3047.
[53] J. B. Chaires, N. Dattagupta, D. M. Crothers, *Biochemistry* **1982**, *21*, 3933.
[54] G. Cohen, H. Eisenberg, *Biopolymers* **1969**, *8*, 45.
[55] H. Y. Ding, X. S. Wang, L. Q. Song, J. R. Chena, J. H. Yu, C. L., B. W. Zhang, *J. Photochem. Photobiol. A: Chem.* **2006**, *177*, 286.
[56] M. J. Frisch, G. W. Trucks, H. B. Schlegel, G. E. Scuseria, M. A. Robb, J. R. Cheeseman, V. G. Zakrzewski, J. A. Montgomery Jr., R. E. Stratmann, J. C. Burant, S. Dapprich, J. M. Millam, A. D. Daniels, K. N. Kudin, M. C. Strain, O. Farkas, J. Tomasi, V. Barone, M. Cossi, R. Cammi, B. Mennucci, C. Pomelli, C. Adamo, S. Clifford, J. Ochterski, G. A. Petersson, P. Y. Ayala, Q. Cui, K. Morokuma, N. Rega, P. Salvador, J. J. Dannenberg, D. K. Malick, A. D. Rabuck, K. Raghavachari, J. B. Foresman, J. Cioslowski, J. V. Ortiz, A. G. Baboul, B. B. Stefanov, G. Liu, A. Liashenko, P.

Piskorz, I. Komaromi, R. Gomperts, R. L. Martin, D. J. Fox, T. Keith, M. A. Al-Laham, C. Y. Peng, A. Nanayakkara, M. Challacombe, P. M. W. Gill, B. Johnson, W. Chen, M. W. Wong, J. L. Andres, C. Gonzalez, M. Head-Gordon, E. S. Replogle, J. A. Pople, GAUSSIAN98, Revision A.11.4, Gaussian Inc., Pittsburgh PA, 2002.

[57] A. D. Becke, *J. Chem. Phys.* **1993**, *98*, 1372.

[58] A. Görling, *Phys. Rev. A* **1996**, *54*, 3912.

[59] P. Hohenberg, W. Kohn, *Phys. Rev. B* **1964**, *136*, 864.

[60] J. B. Foresman, E. Frisch, 'Exploring Chemistry with Electronic Structure Methods', 2nd edn., Gaussian Inc., Pittsburgh, PA, 1996.

[61] P. J. Hay, W. R. Wadt, *J. Chem. Phys.* **1985**, *82*, 270.

[62] W. R. Wadt, P. J. Hay, *J. Chem. Phys.* **1985**, *82*, 284.

[63] A. Juris, V. Balzani, F. Barigelletti, S. Campagna, P. Belser, A. V. Zelewsky, *Coord. Chem. Rev.* **1988**, *84*, 85.